Refinement of the Structural Phase Diagram for Calcium-doped $RMnO_3$ (R = rare earth)

H. A. Salama, N. S. McLean, N. B. Moyle and G. A. Stewart

School of Physical, Environmental & Mathematical Sciences, University of New South Wales, Australian Defence Force Academy, Canberra, Australia 2600.

An XRD study of a range of $Y_{1-x}Ca_xMnO_3$ and $Yb_{1-x}Ca_xMnO_3$ compounds verifies that the lever law holds for the mixed hexagonal/orthorhombic phase region. However, critical Ca concentrations determined for the respective boundary orthorhombic phases are larger than expected, a phenomenon that is attributed to ionic radius disorder of the Ca^{2+} and trivalent rare earth ions.

1. Introduction

The rare earth manganites continue to attract the attention of researchers, most recently due to their intriguing multiferroic behaviour [1]. With decreasing rare earth ionic radius the structure of the pure manganites ($RMnO_3$, R = rare earth) moves from the orthorhombic $GdFeO_3$-type with space group Pnma (R = La – Tb) to the hexagonal $LnMnO_3$-type with space group $P6_3cm$ (R = Dy – Lu, Y). The hexagonal structure can be converted entirely back to orthorhombic by substituting the trivalent rare earth ion with the larger divalent Ca^{2+} ion, as long as its concentration exceeds a critical (R-dependent) fraction, x_C. Although the structure of under-doped specimens is often referred to in the literature simply as "hexagonal", they are clearly a mixture of pure hexagonal and critically-doped orthorhombic phases. We recently observed this behaviour for a specimen of nominal stoichiometry $Yb_{2/3}Ca_{1/3}MnO_3$ [2]. The only systematic quantitative phase analysis of the mixed phase region that we are aware of is due to Vega *et al* [3] for $Y_{1-x}Ca_xMnO_3$. However, the published phase proportions deviate markedly from the expected "lever law" behaviour. We report here on an x-ray powder diffraction (XRD) study of a range of $Y_{1-x}Ca_xMnO_3$ and $Yb_{1-x}Ca_xMnO_3$ stoichiometries.

2. Experimental Details

Specimens with nominal stoichiometries of $Y_{1-x}Ca_xMnO_3$ (x = 0.05, 0.01, 0.15, 0.2 and 0.25) and $Yb_{1-x}Ca_xMnO_3$ (x = 0.05, 0.2, 0.25 and 0.33) were prepared from Y_2O_3 (99.99%), Yb_2O_3 (99.99%), $CaCO_3$ (99.9%) and $MnCO_3$ (99.9+ %) via repeated solid state reaction in air at 1200 °C. All specimens were oven-cooled to ambient temperature over a period of about 12 hours.

XRD patterns were recorded at room temperature using Cu K_α radiation and Rietveld analyses were performed using the *Rietica* front end for Windows [4] To this end, the atomic position parameters for the hexagonal phases ($YMnO_3$ and $YbMnO_3$) were adopted from the single-crystal XRD work of Van Aken *et al* [5]. Those for the critically-doped orthorhombic phases were estimated from the neutron diffraction work of Blasco *et al* [6] via extrapolation against $\langle r_{R\text{-}Ca} \rangle$, the mean R-Ca site atomic radius [7]. Relative masses of the two phases were estimated from their respective products *SVZM*, where *S* is the fitted Rietveld scale factor for the phase, *V* is its unit cell volume, *Z* is the number of formula units per unit cell and *M* is the molecular weight for the formula unit [8]. According to the lever law, the theoretical weight percent of the orthorhombic boundary phase is given by

$$w_O = 100\, x M_{\mathrm{O}} / \left[(x_C - x) M_{\mathrm{H}} + x M_{\mathrm{O}} \right] \qquad (1)$$

3. Results

The sets of XRD patterns are shown in Fig. 1. In each case, the orthorhombic boundary phase's reflections are seen to grow at the expense of the hexagonal phase reflections as the nominal Ca fraction is increased.

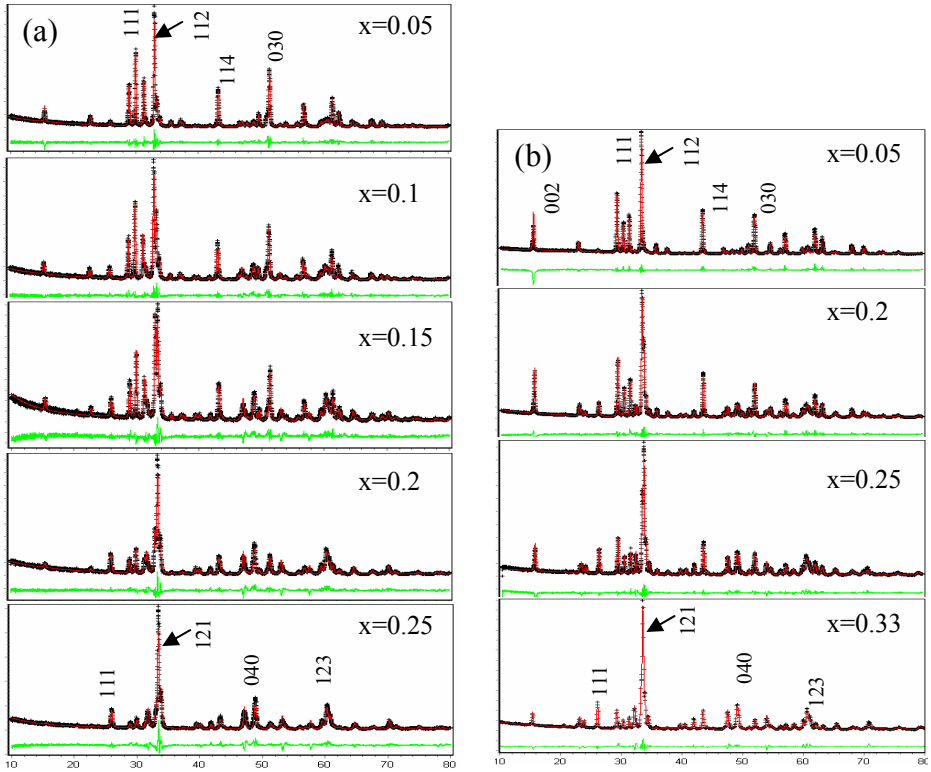

Fig. 1. X-ray diffraction patterns recorded with CuK_α radiation at room temperature for the nominal specimen stoichiometries of (a) $Y_{1-x}Ca_xMnO_3$ and (b) $Yb_{1-x}Ca_xMnO_3$. The lines beneath the plots indicate the difference between the data and the fitted theory curve. The labelled reflections for x = 0.05 and for x = 0.25, 0.33 refer to the hexagonal and orthorhombic phases, respectively.

In Fig. 2 the experimental weight percent of the orthorhombic boundary phase is shown as a function of the nominal Ca fraction. From a straightforward extrapolation to 100 %, it

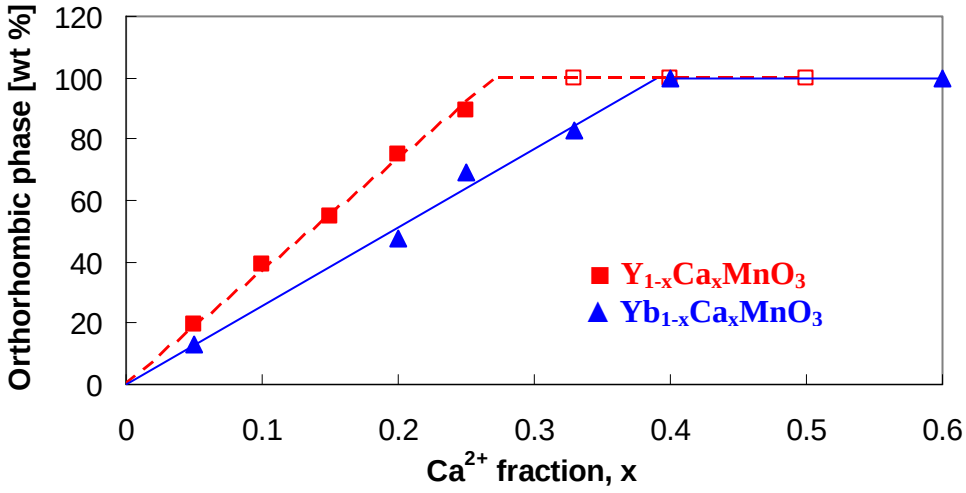

Fig. 2. Experimental wt% of the orthorhombic boundary phase for the nominal specimen stoichiometries $Y_{1-x}Ca_xMnO_3$ and $Yb_{1-x}Ca_xMnO_3$.

Table 1. Critical concentration x_C, mean ionic radius $<r_{R\text{-}Ca}>$, tolerance t and variance $\sigma_{R\text{-}Ca}^2$ for the boundary orthorhombic phases of $Y_{1-x}Ca_xMnO_3$ and $Yb_{1-x}Ca_xMnO_3$

R	Method	x_C	$<r_{R\text{-}Ca}>$ [nm]	t	$\sigma_{R\text{-}Ca}^2$ [10^{-8} nm^2]
Y	Extrapolation	0.272(4)	0.1104(1)	0.8774	2183
	Lever law	0.268(4)	0.1103(1)	0.8771	2163
Yb	Extrapolation	0.391(12)	0.1906(2)	0.8807	4535
	Lever law	0.372(11)	0.1903(2)	0.8788	4449

was possible to estimate the critical fraction, x_C. An alternative approach was to plot the experimental weight percent of the orthorhombic phase against its theoretical, lever law weight percent according to Equ. (1). The x_C values were then adjusted until the fitted trend-lines passed through (100%, 100%). Because the Bragg intensities for the boundary orthorhombic phase are expected to be influenced by its Ca content and the concomitant variation of its atomic position parameters, the XRD analyses were repeated for each new x_C value. This process was continued until self consistency was achieved. However, it was found that small changes (less than 10%) in x_C exerted very little influence on the final result.

The two different estimates of x_C are recorded in Table 1 for each of the specimen sets, together with their corresponding $<r_{R\text{-}Ca}>$, tolerance, $t = (<r_{R-Ca}> + r_O)/\sqrt{2}(<r_{Mn}> + r_O)$, and variance $\sigma_{R-Ca}^2 = <r^2> - <r>^2$. Tolerance is commonly employed in the literature as an indicator of structural stability, with $t = 1$ corresponding to the ideal cubic perovskite structure and $\sigma_{R\text{-}Ca}^2$ is a measure of the size disorder of ions occupying the rare earth site.

4. Phase boundary

In Fig. 3, the structures of Ca-doped manganites are represented on a field of x versus the trivalent rare earth radius. Orthorhombic structures are indicated by squares, hexagonal by solid diamonds and mixed hexagonal/orthorhombic by open diamonds. As a first attempt, it was assumed that the critical radii for $Y_{1-x_c}Ca_{x_c}MnO_3$ and $Yb_{1-x_c}Ca_{x_c}MnO_3$ will apply for all other systems. The average of the two values was then employed to define the mixed-phase $\leftrightarrow$ orthorhombic phase boundary (solid line in Fig. 3). Also included as dotted lines are the boundaries predicted for doping with the larger Sr^{2+} and Ba^{2+} ions. However, it is evident from Fig. 3 that the critical radii for $Y_{1-x_c}Ca_{x_c}MnO_3$ and $Yb_{1-x_c}Ca_{x_c}MnO_3$ are too dissimilar for their average value to be used for this purpose. The solid boundary line passes well below the x_C value for the $Y_{1-x}Ca_xMnO_3$ system and well above the value for $Yb_{1-x}Ca_xMnO_3$. It also intersects the horizontal axis between the locations of the undoped $GdMnO_3$ and $DyMnO_3$, whereas it is commonly assumed that the boundary should lie closer to $DyMnO_3$ at $r \geq 0.1076$ nm or $t \geq 0.857$. As a guide to the eye, the hand-drawn, broken line in Fig. 3 would provide a more appropriate representation of the phase boundary based on our present data. That is, the critical x_C (and the corresponding $<r_{R\text{-}Ca}>$ and t values) increase as we move from the undoped host through to the doped $Yb_{1-x}Ca_xMnO_3$ system.

A similar effect was observed by Bos *et al* [9] for the system $Y_{1-x}Gd_xMnO_3$ and the authors attributed it to size disorder of the ionic radii. In the inset of Fig. 3, the critical t values determined here for the two systems are plotted against the corresponding $\sigma_{R\text{-}Ca}^2$ values. Also included in the plot are the pure host data point ($\sigma^2 = 0$, $t \approx 0.857$) and the data point (289, 0.862) determined for $Y_{1-x}Gd_xMnO_3$ [9]. By comparison the present variance values are much larger than that for $Y_{1-x}Gd_xMnO_3$. These data lend support for the influence of size.

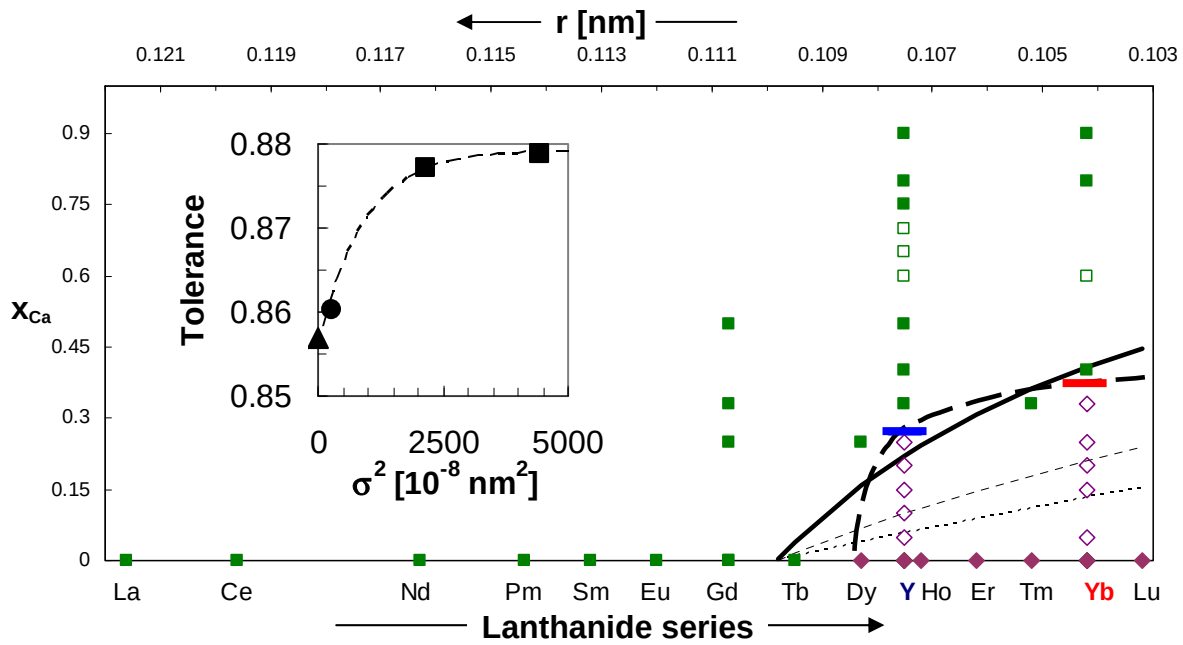

Fig. 3. Structural phase diagram for $R_{1-x}Ca_xMnO_3$ with boundaries as described in the text. Square/diamond symbols represent orthorhombic/ hexagonal structures, with open symbols signifying mixed phase regions.

disorder but further critical parameters for a mid-range $\sigma_{R\text{-}Ca}^2$ (R = Dy-Y?) value would strengthen the case.

5. Conclusion

In conclusion, lever law behaviour has been confirmed for mixed-phase specimens of nominal stoichiometry $Y_{1-x}Ca_xMnO_3$ and $Yb_{1-x}Ca_xMnO_3$, and the critical Ca concentrations for the formation of a 100 wt% $GdFeO_3$-type, orthorhombic structure have been determined in each case. The consistency of the experimental data supports the assumption that the solubility of Ca in the hexagonal phases of $YMnO_3$ and $YbMnO_3$ is negligibly small. It is very likely that the x_C values are inflated by increasing R-Ca ionic size disorder.

Acknowledgments

Hazar Salama gratefully acknowledges her University International Postgraduate Award and University College Postgraduate Research Scholarship.

References

[1] Y.H. Huang, H. Fjellvag, M. Karpinnen, B.C. Hauback, H. Yamauchi and J.B. Goodenough, Chem. Mater. 18, 2130 (2006).

[2] H.A. Salama, D. Scott, J.B. Taboada, N. Strickland, H. O'Neill & G.A. Stewart, Proceedings of the 31st Annual Condensed Matter & Materials Meeting, Wagga Wagga, 2007 (On-line publication, AIP web site).

[3] D. Vega, G. Polla, A.G. Leyva, P. Konig, H. Lanza, A. Esteban, H. Aliaga, M.T. Causa, M. Tovar and B. Alascio, *J. Solid State. Chem.* 156, 458 (2001).

[4] B.A. Hunter and C.J. Howard, Rietica 2000. [available from: www.ccp14.ac.uk].

[5] B.B. Van Aken, A. Meetsma and T.T.M. Palstra, arXiv:cond-mat/0106298v1 (2001).

[6] J. Blasco, J. Garcia, J.M. de Teresa, M.R. Ibarra, P.A. Algarabel and C. Marquina, J. Phys.: Condens. Matter 8, 7427 (1996).

[7] R.D. Shannon, Acta Cryst. A 32, 751 (1978).

[8] R.A. Young, 1993. The Rietveld method. Oxford University Press, New York.

[9] J-W.G. Bos, B.B. van Aken and T.T.M.Palstra, Chem. Mater. 13, 4804 (2001).